

Aircraft Carrier Multipath Modeling for Sea-Based JPALS

Jan P. Weiss, Steve Anderson, Corey Fenwick, Lin S. Stowe, Penina Axelrad
Colorado Center for Astrodynamics Research, University of Colorado, Boulder
Sean M. Calhoun, Richard P. Pennline
ARINC Engineering Services, LLC

BIOGRAPHY

Jan P. Weiss is a Ph.D. candidate in the Department of Aerospace Engineering Sciences at the University of Colorado, Boulder. His research focuses on ground and airborne platform GNSS multipath simulation and analysis as well as antenna and receiver based techniques for multipath detection/mitigation. He received his B.S. in Physics from Creighton University and M.S. in Aerospace Engineering Sciences from the University of Colorado.

Steve Anderson is a Professional Research Assistant with the Colorado Center for Astrodynamics Research at the University of Colorado, Boulder. He received his M.S. in Electrical and Computer Engineering from the University of Colorado and B.S. in Electrical Engineering from the University of North Dakota. He has been involved in GPS research and programs since 1992.

Corey Fenwick is a graduate student at the University of Colorado, Boulder seeking an M.S. degree in Aerospace Engineering Sciences. Currently, he is a research assistant at the Colorado Center for Astrodynamics Research. In 2004, he graduated from the University of Kansas with a B.S. in Aerospace Engineering.

Lin S. Stowe is a graduate student in the Department of Aerospace Engineering Sciences at the University of Colorado, Boulder. Her research interests include GPS multipath studies and ambiguity resolution for carrier phase based navigation solutions. She completed her undergraduate studies in Physics and Computer Science at Rensselaer Polytechnic Institute.

Penina Axelrad is a Professor of Aerospace Engineering Sciences at the University of Colorado, Boulder. Her research is focused on GPS technology and data analysis for aerospace applications. She has been involved in GPS-related research since 1985, previously at Stanford University and Stanford Telecommunications, Inc.

Sean M. Calhoun is a Senior Engineer with ARINC Engineering Services, LLC. Mr. Calhoun received his B.S. in Electrical Engineering, Physics, and Mathematics from Ohio University.

Richard P. Pennline is a Principal Engineer with ARINC Engineering Services, LLC. He is currently responsible for the flight test demonstration system in support of research and development efforts for the Joint Precision Approach and Landing System (JPALS). He has twenty years experience in research, development, test, and evaluation of GPS, space, and communication systems. Mr. Pennline received his B.S. in Electrical Engineering from Carnegie Mellon University.

ABSTRACT

This paper provides an overview of multipath modeling for the Sea-Based Joint Precision and Landing System (JPALS). The model integrates a detailed structural model of the aircraft carrier USS Eisenhower, receiving antenna gain and phase patterns, receiver tracking loop models, and satellite motions to simulate both code and carrier phase tracking errors due to multipath. These efforts complement analysis of actual shipboard test data [2] and use one dockside data set for model validation. For this purpose, a top-level yardarm antenna/receiver system is simulated and the multipath results are compared to actual test data. Comparisons are given in the form of code multipath time histories and elevation dependent error statistics. The statistical comparisons show that the model accurately captures elevation-dependent elevation error magnitudes and trends. Simulated carrier phase multipath results show $1-\sigma$ magnitudes of under 0.5 cm and maximum errors of less than 1.5 cm.

The Advanced GNSS Multipath Model is also used to evaluate expected performance of fixed and beam-steering controlled radiation pattern antennas located on both the top and middle levels of the yardarm structure. The results show higher levels of multipath at the middle

yardarm location, primarily due to additional multipath reflections/diffractions from the top yardarm. Improved multipath performance with beam-steering antenna is demonstrated on both yardarm levels.

INTRODUCTION

The Sea-Based (SB) Joint Precision Approach and Landing System (JPALS) is the next generation military GPS-based system for landing aircraft on ships. It is envisioned that SB JPALS will support autoland operations even under zero visibility conditions. This requires sub-meter accuracy position solutions and necessitates the use of carrier phase-based kinematic positioning [4, 7].

The stringent SB JPALS accuracy requirements make it imperative to minimize and thoroughly understand all possible error sources. One of the significant error sources for the shipboard platform is multipath on both carrier phase and code measurements. Code multipath errors are important because pseudorange measurements are used to limit the carrier phase ambiguity search space. Large pseudorange errors lead to a correspondingly large range of possible integer ambiguities. Furthermore, if the pseudorange uncertainty is underestimated, it can lead to incorrect integer solutions. Carrier phase multipath errors are much smaller in magnitude (on the order of a few cm) than code multipath but can still preclude reliable ambiguity resolution in high multipath environments. If integers are correctly resolved, carrier phase multipath, along with other error sources such as tropospheric delay and ship structure flexure, still contributes to the overall positioning error budget.

One way to characterize and understand multipath errors for the complex shipboard environment is by way of a model. Our efforts rely on a GNSS Multipath Model [10] which integrates reflector environment geometries, satellite almanac data, and antenna/receiver models to simulate multipath errors. The complete model is comprised of five modules. The satellite motion module uses almanac or ephemeris data to compute satellite locations with respect to the antenna location. The environment module defines the ship structure (i.e., reflector environment) and the material properties of each object. The ray-tracing module determines signal paths from the GPS satellite to the receiving antenna, known as the prediction point, taking into account combinations of signal interactions (reflections, diffractions, and transmissions) with the reflector environment. The ray-antenna module applies the receiving antenna pattern and determines the multipath delay, relative amplitude, and relative phase. Both fixed radiation pattern antennas (FRPA) and controlled radiation pattern antennas (CRPA) may be simulated. Finally, the tracking loop module

simulates the receiver front-end and code and carrier phase tracking loop response to multipath.

This paper provides an overview of several simulated multipath studies for the aircraft carrier USS Eisenhower (CVN 69). These complement concurrent experimental shipboard data analysis which is underway. First, we give an overview of the model in the context of the aircraft carrier simulations and the associated experimental data. Next, model validation results, comparing simulated multipath and 13 hours of live P(Y) code multipath data collected while the ship was in dock, are shown. Third, the ability of the model to predict multipath error levels for different antenna equipment is explored. Here we compare the multipath performance of a 7-element beam-steering antenna array and a choke ring antenna. Finally, some visualization tools that identify reflectors and multipath signal paths in the environment are described.

AIRCRAFT CARRIER MULTIPATH MODEL

This section describes the components of the Advanced GNSS Multipath Model as they pertain to the aircraft carrier simulations. More general descriptions, including details on the MATLAB® software implementation, were presented in [10]. The WinProp ray-tracing software and propagation models are developed by AWE Communications.

Satellite Motion

The satellite motion module defines the satellite tracks for each simulation. Here, the tracks are taken directly from the experimental data set described below.

Reflector Environment

The environment module defines the reflector environment. The aircraft carrier surface geometry was created using AutoCAD 2005® based on scale computer aided design (CAD) drawings provided by the Navy [3]. The ship model is comprised of 744 surfaces, and 4 surfaces were added to represent the dockside and surrounding sea surface. The ship CAD model is shown in Figure 1; Figure 2 shows the complete environment model including the dock and sea surface. For reference, a satellite picture of the actual ship dock location is given in Figure 3. Overall we note that the environment model is intended to capture dominant surfaces but certainly ignores smaller objects as well as vehicles, dockside buildings, and other ships.

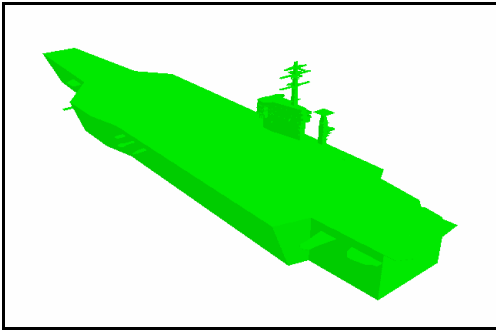


Figure 1: CVN 69 CAD model.

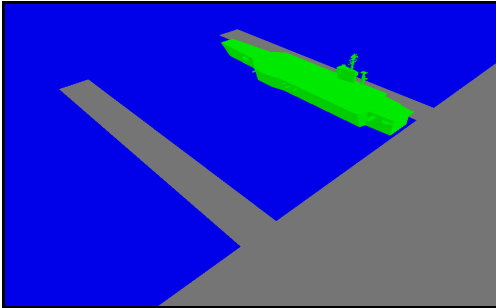


Figure 2: Ship and dock/sea surface model.



Figure 3: Satellite picture of actual dock location. (Photo Google Earth/Digital Globe)

Material properties are defined separately for the ship structures, dock, and ocean surface. These are chosen such that multipath magnitudes seen in the real and simulated data match reasonably well. The material properties which are used for these simulations are summarized in Table 1. We expect to refine these in the future by taking advantage of the fact that the modeled material properties can be adjusted without rerunning ray tracing computations. This is because the ray tracing results depend only on the satellite-reflector geometry and the prediction point. Thus, to adjust a given material property, one only needs to search for rays that interacted with this material. To adjust, for example, the reflection

coefficient, one simply changes the power of the ray at the prediction point. Once the search and adjustments are done, multipath processing is simply started at the ray-antenna module.

Table 1: Aircraft carrier simulation material properties.

Interaction Type	Aircraft Carrier Coefficient	Dock Coefficient	Ocean Surface Coefficient
Transmission	Disabled	Disabled	Disabled
Reflection	0.4	0.18	0.2
Diffraction	0.12 (max)	Disabled	Disabled

Ray Tracing

The ray-tracing module performs the electromagnetic ray tracing computations. The transmitters that represent the GNSS satellites are defined automatically by a MATLAB function that converts satellite azimuths/elevations to the appropriate XYZ coordinates relative to the prediction point. For each satellite epoch, the ray tracing algorithm reports results in the form of the impulse response (time of arrival, power), ray travel paths, ray interactions, and surface/material IDs at which each interaction occurred. This information allows us to compute all multipath parameters and keep track of reflection from the ocean surface. We currently compute rays with up to 2 interactions. These results are then passed to the ray-antenna module.

Ocean surface reflections may also be accounted for separately by way of a rough surface model for GPS scattering from the ocean [11]. This model modifies the ranging code correlation function according to ocean surface wind speed. In our implementation, the user simply chooses an ocean reflection correlation function from a library that contains correlations for a set of common wind speeds. The tracking loop functions then use a delayed and scaled ocean surface correlation instead of a scaled/delayed replica of the direct signal correlation for signals which reflected from the ocean. In general, the ocean correlation function differs from the direct in that the trailing edge of the triangle is distorted due to diffuse scattering. This effect is, however, negligible in these simulations for two reasons. First, the distortion of the correlation peak is only very minor for the yardarm antenna height above the ocean (about 60 m). Second, almost all multipath signals result from interaction with the aircraft carrier so the effect of ocean surface is very minor.

Ray-Antenna Module

The ray-antenna model reads the ray-tracing outputs and converts them to standard GNSS multipath parameters. These are delay relative to the direct signal, relative phase (includes geometric delay, polarization, and antenna phase pattern), and relative amplitude (includes interaction losses and antenna gain pattern).

The FRPA model used for model validation is based on anechoic chamber measurements for the Sensor Systems S-96 series choke-ring antenna used during the ship test [8]. The pattern data include right-hand circular polarization (RCP) and left-hand circular polarization (LCP) gain and phase at the L1 frequency. These pattern data are accessed in the simulation by way of a gain/phase lookup for a given angle of arrival and polarization. A sample cut of antenna gain pattern is shown in Figure 4.

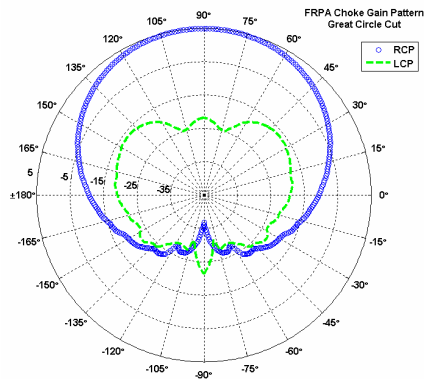


Figure 4: Vertical cut of choke-ring antenna gain.

Receiver Tracking Module

The tracking loop model is a MATLAB implementation of standard uncoupled code and carrier phase tracking loops [6].

EXPERIMENTAL DATA

The experimental data were collected on the USS Eisenhower in the spring of 2005. For model validation we use one ~13 hour data set collected while the ship was docked. The GPS receiver tracked dual frequency P(Y) code and carrier phase and was connected to a Sensor Systems S-96 series L1/L2 choke-ring antenna. The antenna was mounted on the top yardarm marked with an arrow in Figure 5. Embedded GPS/Inertial navigation system data are used to transform satellite azimuth/elevation into the aircraft carrier body frame. This step is required to capture the satellite-reflector geometries correctly. The body frame satellite sky plot is given in Figure 6. For further details on the experimental data collection effort the reader is referred to Reference 2.



Figure 5: Aircraft carrier island showing yardarm where antenna is mounted.

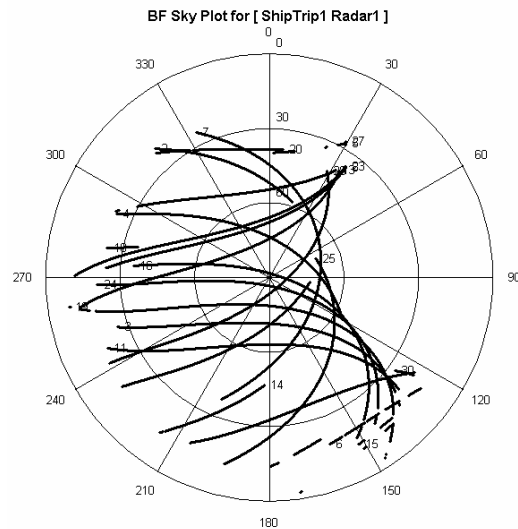


Figure 6: Body frame satellite sky plot.

MODEL VALIDATION

To validate the model we compare real and simulated code multipath data in the form of time histories and overall error statistics. To make meaningful comparisons the simulated and real receiver parameters are matched as closely as possible as shown in the table below.

Table 2: Receiver system summary.

Receiver System Parameter	Real Receiver	Simulated Receiver
Antenna	S-96 choke-ring	S-96 choke-ring
Frequency	L1 / L2	L1
Code Type	P(Y)	P
Correlator Spacing	1.0 chips	1.0 chips
Front-end Bandwidth	Unknown	20 MHz
Data Recording Rate	1 Hz	1/10 Hz

Code Multipath Results

The figures below show several real and simulated code multipath time histories. At times the multipath errors track one another well in terms of both frequency and amplitude, and at other times there are mismatches. For example, the multipath frequencies in Figure 8 agree for much of the satellite pass, but simulated magnitudes before 6.5 hours are smaller than those seen in the real data. Mismatches are not surprising since the simulation does not capture several factors which contribute to multipath. First, the ship CAD model does not capture small objects on ship. Also, the simulated environment does not include some static structures or moving equipment. This includes ships and buildings on the surrounding dockside, equipment on the deck of the aircraft carrier (aircraft, flight support and maintenance vehicles), as well the operation of elevators and blast deflectors on the deck. Furthermore, the simulations do not model low signal power tracking problems (such as cycle slips) which occur in the real data, especially at lower elevations where the choke-ring strongly attenuates incoming signals. Finally, the installed choke-ring antenna pattern will differ slightly from the anechoic chamber measurements.

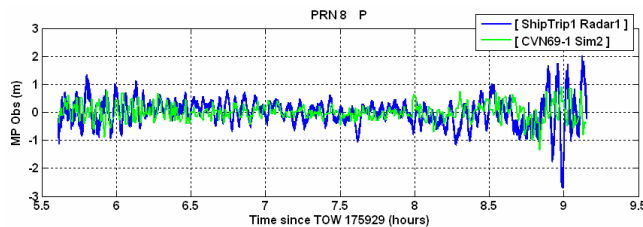


Figure 7: Comparison of real and simulated code multipath, PRN 8.

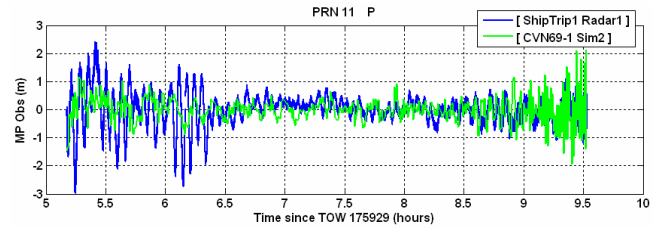


Figure 8: Comparison of real and simulated code multipath, PRN 20.

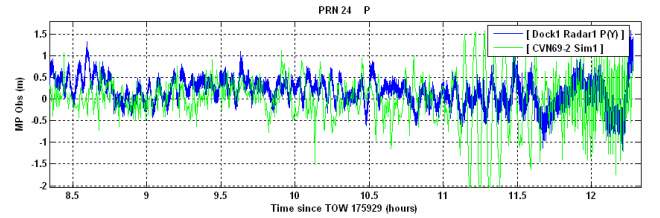


Figure 9: Comparison of real and simulated code multipath, PRN 11.

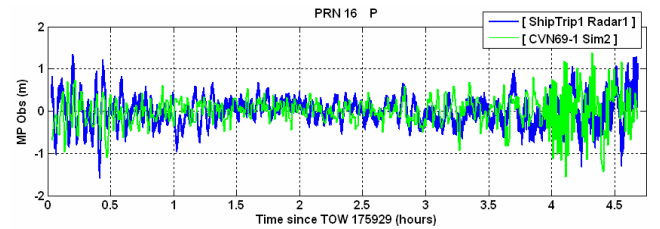


Figure 10: Comparison of real and simulated code multipath, PRN 16.

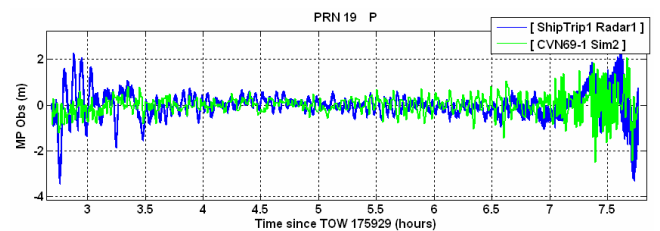


Figure 11: Comparison of real and simulated code multipath, PRN 19.

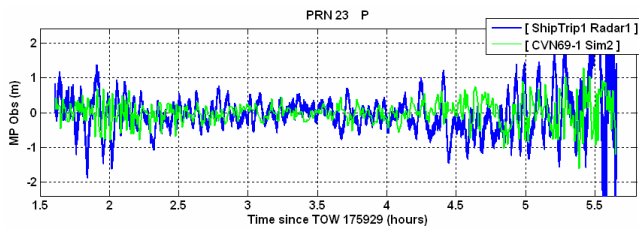


Figure 12: Comparison of real and simulated code multipath, PRN 23.

Overall multipath statistics also assess how well the simulated multipath matches the live data. The overall multipath $1-\sigma$ statistics per 10 degree elevation bin are shown in Figure 13, where the left and right set of bars show the real and simulated multipath statistics, respectively. This comparison shows that the model captures multipath quite well in the statistical sense. Overall, the model not only correctly predicts the trends across the elevation bins but also predicts the $1-\sigma$ magnitudes to within 90% across all bins.

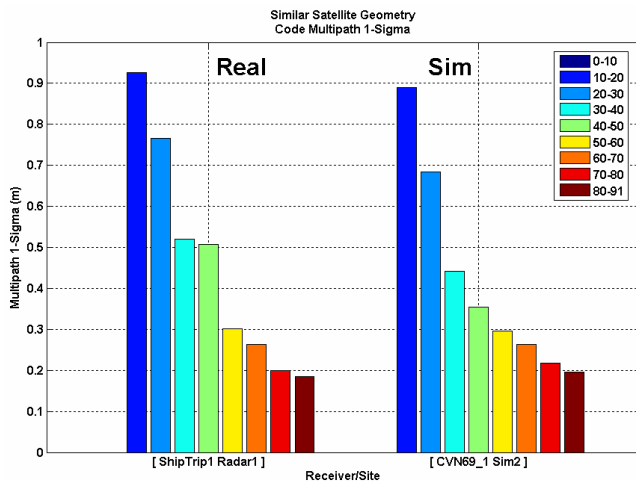


Figure 13: Real and simulated aircraft carrier code multipath $1-\sigma$ statistics.

Carrier Phase Multipath Results

The model also computes carrier phase error due to multipath directly for a given site. This is advantageous because carrier phase multipath cannot be isolated in live measurements. Double-difference or inter-frequency carrier phase multipath observables always contain a combination of multipath from two sites and two different satellites or frequencies [2]. The simulated carrier phase multipath $1-\sigma$ statistics corresponding to the validated code multipath are shown in Figure 14. It is promising that $1-\sigma$ magnitudes are well below 1 cm. The model predicts that maximum carrier phase errors for this

satellite geometry are no larger than 1.5 cm, as shown in Figure 15.

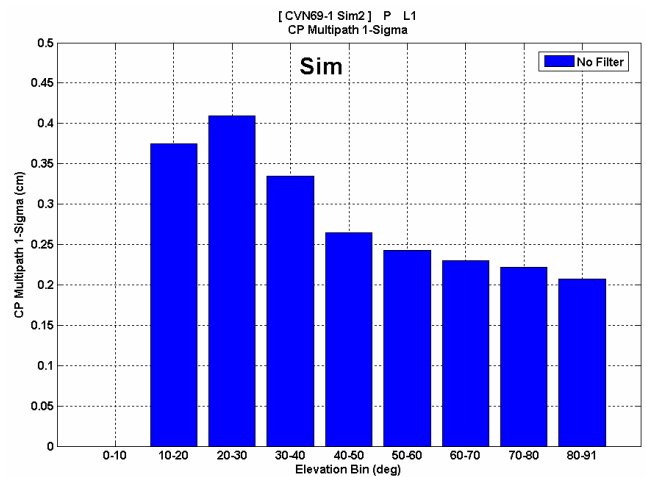


Figure 14: Carrier phase multipath $1-\sigma$.

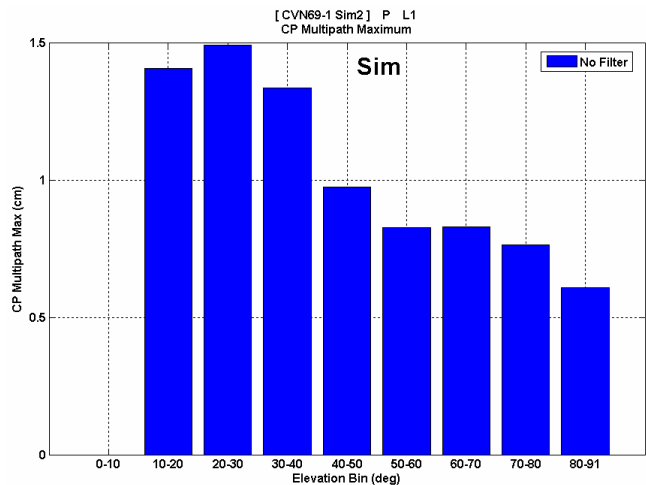


Figure 15: Carrier phase multipath maximum.

Computational Costs

The computational cost of a given simulation depends upon a number of factors driven by the ray-tracing, antenna models, and tracking loops. For ray-tracing, these factors include the environment complexity and number of surfaces, the number of interactions to consider, the number of transmitters (i.e., number of epochs per satellite), and the number of prediction points (receiving antennas). After ray-tracing is completed, the antenna pattern is applied and the ray-tracing outputs are converted to multipath parameters. This step is fastest with an omni-directional antenna, but slows down when using a FRPA or CRPA due to the required gain/phase lookups and/or weighting matrix calculations. The code and carrier tracking loop models are mostly affected by the precision to which the multipath delays are computed.

This affects the simulation speed because the code correlation functions must be sampled to this precision, so an increase in precision from 1 cm to 1 mm will result in correlation function vectors which are ten times as long. We have found that 1 cm precision is a good tradeoff between computational speed and the ability to capture multipath errors with sufficient accuracy.

The simulation tasks and associated computational time for the validation simulation are summarized in Table 3. The breakdown is given for both a single and double interaction simulation corresponding to the 13 hour live data set. Both simulations were run on the same Pentium 4 / 2.8 GHz PC. The double interaction results were of course used because they represent the live data much more accurately. The increased accuracy comes at a much higher computational expense, though, as the total simulation time increased by about a factor of 70. While the total simulation time is still acceptable in this case, we are currently exploring the use of additional processors as well as the distribution of tasks to multiple PCs via a local area network.

Table 3: Computational tasks for aircraft carrier validation simulation.

Computational Task	Aircraft Carrier @ One Interaction	Aircraft Carrier @ Two Interactions
MATLAB file I/O	10 min	150 min
Ray Tracing	30 min	7700 min
Apply Antenna Pattern	15 min	40 min
Code/Carrier Tracking Loops	45 min	250 min
Total:	~2 hours	~137 hours

COMPARATIVE MULTIPATH PERFORMANCE STUDIES

One important application of this multipath model is the evaluation of expected multipath error for different antenna types and locations in a given environment. Such studies can be very helpful in identifying candidate antenna equipment and sites which reduce overall multipath error. In the context of the aircraft carrier, the expected performance of beam-steering CRPA equipment and the level of multipath on the middle yardarm are of interest.

Sample results for a beam-steering antenna are shown next. This simulation uses a 7-element GPS Antenna System 1 (GAS 1) CRPA model provided by Rockwell

Collins [1,5]. This antenna model utilizes spatial adaptive processing (SAP) only and the geometry of the array is shown in Figure 16. A weighted sum of the outputs of each of the antenna elements is computed to create a composite antenna pattern that can be controlled to enhance direct and attenuate multipath signals. In our implementation, the RCP and LCP antenna patterns for each element are only loaded once while the weighting algorithms and gain/phase lookups are performed at each epoch. To improve computational performance, the composite gain/phase pattern are computed only for angles at which signal rays are present (rather than for the complete pattern).

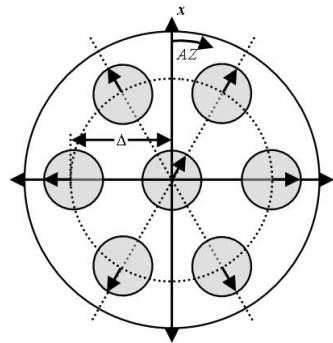


Figure 16: GAS-1 CRPA diagram. Courtesy of Rockwell Collins.

The CRPA performance is evaluated for two sample satellites by comparing CRPA multipath to a non-choke ring FRPA at the top-level yardarm location. Since this is a comparison of simulated data only, receiver noise is not included in the multipath observables. Sample time histories are shown below. As one can see, the beam-steering CRPA is able to reduce multipath because the antenna array applies positive gain towards the direct signal while attenuating multipath signals arriving from other directions. It is notable that at certain times, such as between hours 5-6 in Figure 17 and hours 10.5-11 in Figure 18, the CRPA errors are comparable to those of the FRPA. This is not unexpected since the composite CRPA pattern sometimes exhibits “parasitic beams” where arriving signals are not significantly attenuated [5,9]. An example of a composite CRPA pattern with parasitic beams is given in Figure 19. Here the pattern is steering towards an azimuth of 90 deg but one can see that signals arriving from azimuths around 220 deg and 320 deg would not be significantly reduced by the antenna.

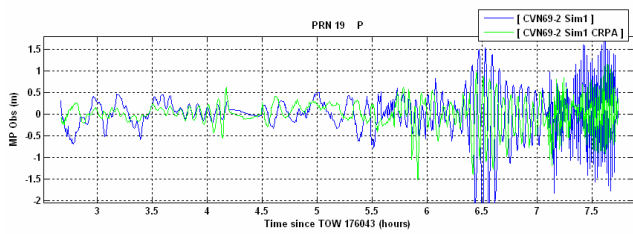


Figure 17: Comparison of simulated FRPA/CRPA multipath, PRN 19.

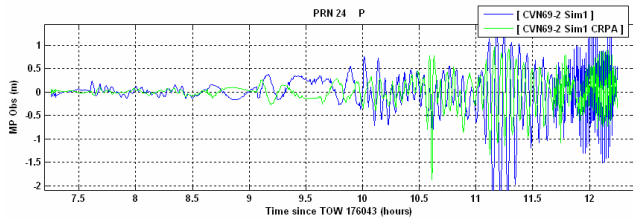


Figure 18: Comparison of simulated FRPA/CRPA multipath, PRN 24.

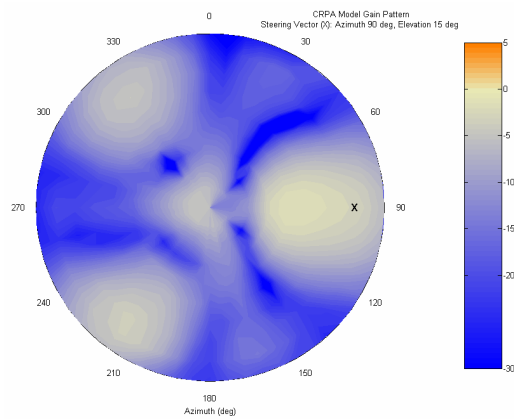


Figure 19: Modeled upper-hemisphere CRPA gain pattern for azimuth 90° / elevation 15°.

The model is also a powerful tool for comparing relative multipath levels at various locations. This is useful because it is not practical to install and test equipment at all candidate locations for a specific installation. In the case of the aircraft carrier, space for antenna equipment was limited to the top yardarm for the spring 2005 tests described above. But what is the expected multipath if antennas could be placed on the middle yardarm? To answer this question, a simulation is run with identical conditions except that the receiving antenna is moved 3.8 m lower to just above the middle yardarm. Results for a sample of five identical satellite tracks are shown below. Figure 20 shows a multipath time history (no noise) and one can see that the middle yardarm tends to have larger

errors. There is also a data outage for the middle yardarm due to direct signal blockage from the top yardarm. This makes sense because the middle yardarm will experience multipath not only from the ship below but also from the mast and equipment above. The statistics for all satellites in Figure 21 confirm this, with significantly larger $1-\sigma$ values above 50 deg.

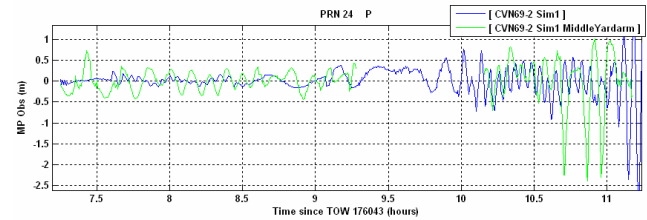


Figure 20: Sample multipath time history for upper/middle yardarm, PRN 24.

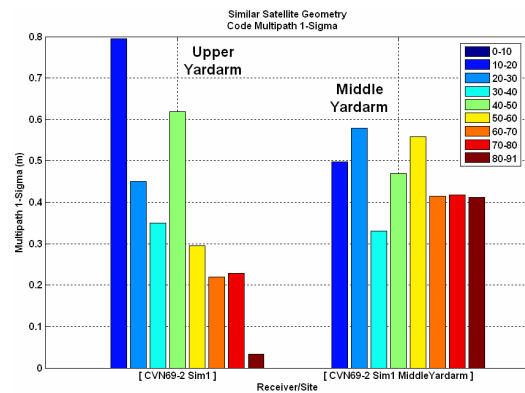


Figure 21: Comparison of upper/middle yardarm multipath statistics for five identical satellite tracks.

VISUALIZATION TOOLS

Several useful multipath visualization tools have also been developed. For instance, multipath error can be plotted alongside the impulse response and angle of arrival information. This allows one to quickly assess how many multipath signals contribute to multipath error at a given epoch as well as the directions of reflectors. The figure below shows a sample multipath impulse response. Here the multipath error for one epoch is highlighted in the top plot while the impulse response and angles of arrival are shown in the bottom plots. The impulse response and angles of arrival are color coded according to whether the final multipath interaction was a diffraction (green) or a reflection (blue). Generally these visualizations are viewed in the form of a movie in order to illustrate the changing interactions between multipath delay, relative amplitude, and total multipath error.

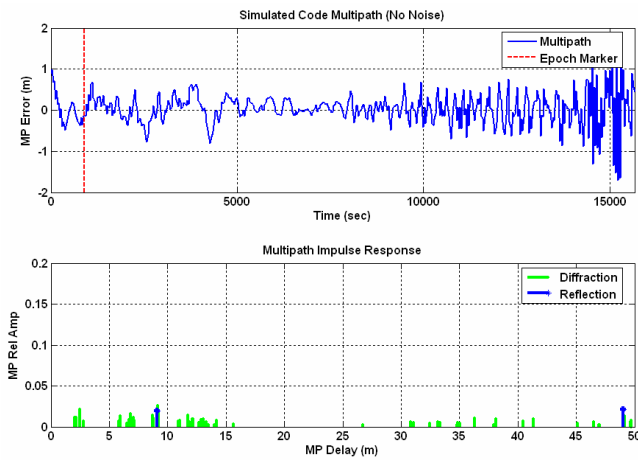


Figure 22: Sample multipath impulse response visualization.

Finally, the multipath model includes a tool to visualize ray paths within the environment model. Figure 23 shows sample ray paths for one satellite epoch with the prediction point marked in blue. One can see the direct signal as well as a few diffractions from the yardarm. While this view does not provide information about multipath delays or relative amplitudes, it often helps to quickly identify multipath geometries. Figure 24 shows the same satellite-reflector geometry and adds second order interactions. This clearly illustrates how each additional interaction and the corresponding geometric complexities contribute to a significantly higher computational burden.

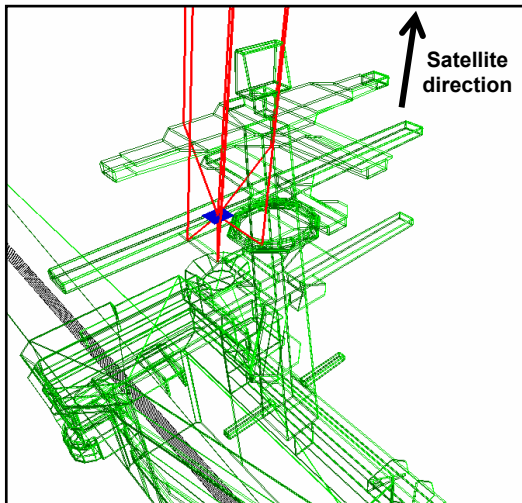


Figure 23: Middle yardarm ray-path example (single interactions).

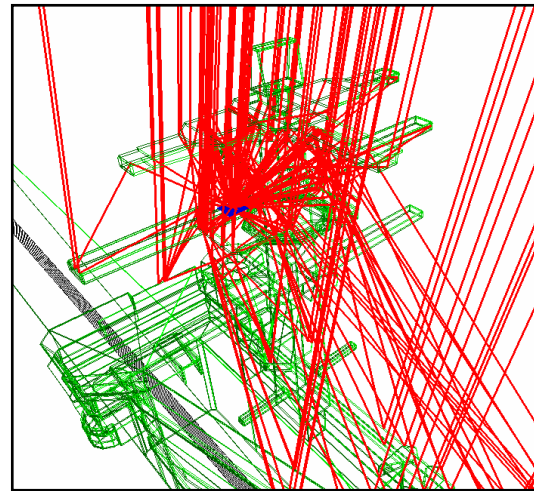


Figure 24: Middle yardarm ray-path example (single and double interactions).

CONCLUSIONS AND FUTURE WORK

A comprehensive GNSS multipath model has been developed and applied to the USS Eisenhower aircraft carrier. The model utilizes a CAD model of the ship structures in combination with 3D ray tracing and detailed antenna and receiver models to predict multipath errors. Model validation was performed by comparing an 13 hours of P(Y) code and carrier phase multipath data collected aboard the ship to simulation results. The receiving antenna location, antenna gain/phase pattern, receiver tracking model, and satellite constellation were set up to represent those of the open-air test as closely as possible. Results presented in the form of multipath time histories and overall error statistic summaries show that the model captures multipath errors accurately. Some discrepancies will always exist, of course, since several simplifications were made in the environment model. In light of these simplifications, however, the multipath model nonetheless shows much promise for reliable and accurate multipath predictions in the shipboard environment. This will complement carrier phase multipath analysis of actual data especially well since the simulation provides unambiguous errors for the site of interest.

Future modeling work to support Sea-Based JPALS is primarily focused on refining the environment models. More comparisons to real data will be made for other antenna locations for both at-sea and dockside data. These simulations will provide additional optimization of the material properties. Also, a highly detailed CAD model of the USS Eisenhower was recently made available. We eventually plan to transition to this model once it has been simplified such that acceptable computational times are realized. Finally, methods for

including ship motions relative to the ocean surface will be investigated.

ACKNOWLEDGEMENTS

The work presented in this article was performed under contract to ARINC Engineering Services, LLC, sponsored by the U.S. Navy Air Systems Command. Gary McGraw and Ryan Young of Rockwell Collins supplied the adaptive beam-steering algorithms used for the CRPA model.

REFERENCES

1. Anderson, Steve, J.P. Weiss, P. Axelrad, R. Pennline. *A GPS Multipath Simulator with Beam-Steering Antenna Modeling for JPALS LDGPS*. Proceedings of the Institute of Navigation's ION GNSS 2004.
2. Anderson, Steve. J.P. Weiss, C. Fenwick, L. Song, P. Axelrad, J. Stevens, R.L. Brinkley, S. Calhoun. *Analysis of P(Y) Code and Carrier Multipath for JPALS Ship and Airborne Receivers*. Proceedings of the Institute of Navigation's ION GNSS 2005.
3. Department of the Navy / Naval Sea Systems Command. *Aircraft Carrier CVN 69 RCOH Antenna Arrangement*. Revision A, May 3, 2004.
4. Department of the Navy / Naval Sea Systems Command. *Systems Requirement Document for Shipboard Relative Global Positioning System Technology Development*. Release 1.0, October 30, 2003.
5. McGraw, Gary A., R. S.Y. Young, K. Reichenauer, J. Stevens, F. Ventrone. *GPS Multipath Mitigation Assessment of Digital Beam Forming Antenna Technology in a JPALS Dual Frequency Smoothing Architecture*. Proceedings of the Institute of Navigation's ION NTM 2004.
6. Misra, Pratap, P. Enge. *Global Positioning System: Signals, Measurements, and Performance*. Lincoln, MA: Ganga-Jamuna Press, 2001.
7. Peterson, Bruce R., G. Johnson, J. Stevens. *Feasible Architectures for Joint Precision Approach and Landing System (JPALS) for Land and Sea*. Proceedings of the Institute of Navigation's ION GNSS 2004.
8. U.S. Navy Air Systems Command (NAVAIR) / Facilities for Antenna and Radar Cross Section Measurements. *JPALS Choke Ring Antenna Measurements Final Report*. June 2005.
9. Weiss, Jan P., S. Anderson, P. Axelrad, R. L. Brinkley, R. P. Pennline. *Analysis of P(Y) Code Multipath for JPALS LDGPS Ground Station and Airborne Receivers*. Proceedings of the Institute of Navigation's ION GNSS 2004.
10. Weiss, Jan P., S. Anderson, C. Fenwick, L. Song, P. Axelrad, P. Belay, R. L. Brinkley. *Development*

- and Validation of an Aircraft Multipath Model for Land-Based JPALS*. Proceedings of the Institute of Navigation's Annual Meeting 2005.
11. Zavorotny, V.U., Voronovich, A.G. *Scattering of GPS Signals from the Ocean with Wind Remote Sensing Application*. IEEE Transactions on Geoscience and Remote Sensing, Vol. 38, No. 2, 2000.